End-Attaching Copolymer Adsorption: Kinetics and Effects of Chain Architecture

J. R. Dorgan† and M. Stamm*

Max-Planck-Institut für Polymerforschung, Ackermannweg 10, D-6500 Mainz, FRG

C. Toprakcioglu

Cavendish Laboratory, Madingley Road, Cambridge CB3 QHE, England

R. Jérôme

Center for Education and Research on Macromolecules, University of Liège, Sart-Tilman B6, 4000 Liège, Belgium

L. J. Fetters

Exxon Research and Engineering Company, Clinton Township, Route 22 East, Annandale, New Jersey 08801

Received March 19, 1993; Revised Manuscript Received June 14, 1993•

ABSTRACT: In this study we report on the adsorption behavior of end-attaching triblock and diblock copolymers. The triblock copolymers consist of relatively short PEO end blocks and a much longer PS middle block or, in one case, of zwitterionic end groups with a PS middle block. The diblock materials consist of a PEO block of fixed length and varying polystyrene lengths. A silicon wafer with an oxide layer is used as the surface, and adsorption takes place from toluene; only the end groups adsorb, leaving the polystyrene block dangling in solution. We find that diblock copolymers which range from symmetric to moderately symmetric obey the scaling law for the surface coverage which was proposed in the theory of Marques and Joanny (i.e., $\sigma \propto 1/N_A$, where N_A is the number of segments in the adsorbing block). However, we find that for triblock copolymers of comparable asymmetry the surface coverage scales according to the relationship $\sigma \propto 1/\beta^2$, where β is the ratio of the size of the nonadsorbing block to that of the adsorbing block. This implies that moderately symmetric triblock copolymers behave like highly asymmetric diblock copolymers; the adsorption behavior is dominated by the nonadsorbing block size. Our experiments demonstrate the observation of extremely long-lived nonequilibrium states. On the basis of these observations we propose a simplified version of a recent theory of adsorption which is capable of qualitatively describing much of the experimentally observed phenomena.

Introduction

The behavior of polymeric materials near a solid interface is very different from the behavior in the bulk because of the existence of strong entropic constraints placed upon the polymer chain conformations near a bounding, impenetrable surface. Theoretical, experimental, and computer simulation studies have been carried out to investigate the structure of polymeric materials near an interface. Polymer coils terminally attached to a solid surface constitute an interface of particular interest. For example, they are used in the stabilization and flocculation of colloidal particles such as those used as precursors to the sintering of ceramics.[1] Uses in biomedical technology include affinity chromatography and the enhancement of biocompatibility of artificial implants. Composite materials consisting of adsorbed polymer chains can be said to represent the ultimate in polymer thin-film technology; a single layer of polymer coils attached to a solid surface. Such thin polymer films are desirable for many applications in electronics and optoelectronics where film properties must be closely controlled.[2] Thin films find widespread use in the microelectronics industry as interlayers in multilayer structures and in the packaging of microelectronics devices.

Polymer molecules are not necessarily attracted to a surface; they may also be nonwetting. In this case there are no favorable stabilizing energetics which attract the polymer to the surface. Recent theoretical and experimental investigations have attempted to quantify the relevant relationships between the energetics of such systems.[3–5] It has been discovered that, below a critical thickness, polymer films may be inherently unstable and thus rupture if brought too near the glass transition temperature. This intrinsic limitation on film thickness provides another strong motivation for the investigation of polymer chains tethered to a surface whereby stabilization can occur.

Many studies have addressed the properties of polymer brushes formed by diblock copolymers at a variety of interfaces, and this subject has recently been reviewed.[6] On the other hand, relatively few studies are available which address the properties of polymer brushes formed from end-attaching triblock copolymer chains.[7,8] In this paper we report on the adsorption behavior of end-attaching triblock and diblock copolymers. The triblock copolymers consist of relatively short PEO end blocks and a much longer PS middle block or, in one case, of zwitterionic end groups with a PS middle block. The diblock materials consist of a PEO block of fixed length and varying polystyrene lengths. A silicon wafer with a well-defined oxide layer is used as the surface, and adsorption takes place from toluene, which dissolves both components. Only the end groups adsorb, leaving the polystyrene block dangling in solution. The conditions employed can thus be said to represent adsorption from a nonselective solvent onto a selective surface.

† Permanent address: Department of Chemical Engineering and Petroleum Refining, Colorado School of Mines, Golden, CO 80401.

• Abstract published in *Advance ACS Abstracts*, September 1, 1993.

0024-9297/93/2226-5321$04.00/0

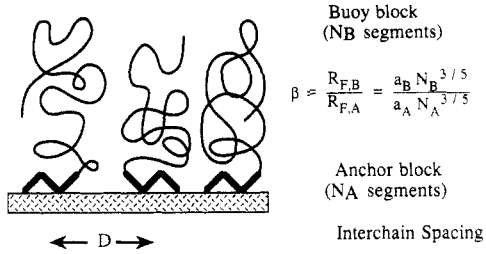

Figure 1. Structure of a copolymer brush. The asymmetry of the copolymer is measured by the ratio of the Flory radius of the nonadsorbing block to that of the adsorbing block. The grafting density, σ, is related to the interchain spacing, D, through $\sigma = D^{-2}$.

There are four principal objectives of the present study: (1) to test the applicability of recently proposed scaling laws for the adsorption of block copolymers, (2) to elucidate the kinetics of the adsorption process, (3) to examine the effects of copolymer architecture on the structure of the adsorbed copolymer layer, and (4) to test the effect of altering the nature of the adsorbing end group. In the background section the relevant definitions and terminology used throughout the work are given. Next, the experimental section details the materials and methods used in our investigation, which is followed by presentation of the results in the following section. A discussion of these results and the conclusions which may be derived from them are the subjects of the final two sections.

Background

For an isolated polymer coil in solution, the natural size of the molecule to consider is the Flory radius, R_F. In a good solvent, the Flory radius scales with the number of repeat units raised to the three-fifths power. This scaling behavior represents a trade-off between the entropic penalty of stretching the coil and its preference to avoid self-interaction and promote polymer–solvent contacts.[9] If a polymer molecule is attached to a solid surface in the presence of other polymer molecules, then the interchain spacing can become less than the Flory radius. In such a situation the chains stretch away from the surface and into the solvent—such a structure is known as a polymer brush.[10-14]

In considering block copolymer adsorption it is necessary to have a measure of the internal composition of the copolymer chains. Both scaling theories and self-consistent field calculations point to the strong dependence of the structure of the adsorbed layer on the relative volume fraction of adsorbing and nonadsorbing blocks.[15-17] We adopt the usual notation of the scaling theories and define the β parameter as the ratio of the size of the nonadsorbing (buoy) block to the size of the adsorbing (anchor) block

$$\beta = \frac{R_{F,B}}{R_{F,A}} = \frac{a_B N_B^{3/5}}{a_A N_A^{3/5}} \quad (1)$$

In eq 1, a_A and a_B represent the segment sizes within the anchor and buoy blocks, respectively, while N_A and N_B represent the number of monomers in each of these blocks. The grafting density of polymer chains at the surface also proves to be an important variable in the description of polymer brushes. The grafting density σ is simply related to the interchain spacing D through $\sigma = D^{-2}$ and represents the number of chains per unit area. A schematic representation of a polymer brush in which these various definitions are illustrated is shown in Figure 1.

In a later part of this paper we attempt to test the scaling laws for copolymer adsorption proposed by Marques and Joanny.[15] These scaling laws have been proposed for diblock copolymer adsorption and predict the existence of three different regimes. However, as pointed out by Guzonas and co-workers, the predicted scaling in two of the three regimes is identical.[18] Accordingly, these authors have suggested a slightly different classification scheme based on the value of β; they identify copolymers where $\beta > N_A^{1/2}$ as highly asymmetric, those for which $1 < \beta < N_A^{1/2}$ as moderately asymmetric, and those for which $\beta < 1$ as symmetric. The crossover at $N_A^{1/2}$ between the moderately asymmetric and highly asymmetric regimes can be identified with the crossover between an adsorption mechanism dominated by the adsorbing block size to one where the nonadsorbing block dictates the surface density. These two mechanism will be referred to as "head" dominated and "tail" dominated, respectively.[19] That is, in the moderately asymmetric regime the grafting density for a given adsorbing block size remains constant with increasing size of the nonadsorbing block. In such a case the grafting density is simply determined by the amount of space each adsorbing "head" block needs on the surface, and nonadsorbing block interactions are negligible. Increasing the size of the nonadsorbing block eventually leads to a regime where tail interactions become dominant; this is the highly asymmetric regime. In this regime, for a fixed adsorbing block size, increasing the nonadsorbing block size leads to a decrease in the grafting density.

Table I. Molecular Characteristics of the Copolymers Used in the Adsorption Studies

material	N_B (PS units)	N_A (PEO units)	$N_A^{1/2}$	β
PEO/PS(17K)/PEO	161	104 (2 × 52)	10.2	1.1
PEO/PS(45K)/PEO	435	86 (2 × 43)	9.3	2.3
PEO/PS(125K)/PEO	1202	10 (2 × 5)	3.2	15.4
PEO(25K)/PS(30K)	288	568	23.8	0.6
PEO(23K)/PS(85K)	817	523	22.9	1.1
PEO(25K)/PS(116K)	1115	568	23.8	1.3
PEO/PS(80K)	730	90	9.5	3.1
PEO/PS(184K)	1700	167	12.9	3.5
PEO/PS(502K)	4788	91	9.5	9.4
Zwit/PS(52K)/Zwit	500	0	N/A	N/A
PEO homopolymer	0	193	N/A	N/A

Experimental Section

Materials. The copolymers used in this study have the molecular characteristics shown in Table I. The triblock copolymers were purchased from Polymer Laboratories, the diblock copolymers with low β values were synthesized at the University of Liège. One of the triblock materials employed had $Na^+SO_3^-$ zwitterionic end groups. Additionally, the characteristics of three previously investigated diblock copolymers from Polymer Laboratories with intermediate β values are shown and will be used for comparative purposes.[20] It can be seen that the materials studied span a large range of β values from a low of 0.6 to a high of 15.4. In calculating these β values, the ratio of monomer sizes has been taken as $a_A/a_B = 0.87$.[18]

Silicon wafers (kindly supplied by Wacker-Chemitronic, Burghausen) with well-defined oxide layers (1200–1600 Å) and a mirror polished finish were used as substrates. The following cleaning procedure was used to ensure the reproducibility of the results: (1) cut wafer pieces held under chloroform were placed in an ultrasonic bath for 15 min, (2) the chloroform is replaced by acetone and the wafers are again subjected to a 15-min ultrasonic bath, (3) the acetone is removed and an aqueous oxidizing solution of a 50:50 mixture of NH_3 and H_2O_2 is allowed to act overnight, (4) the wafers are rinsed in ultrapure water from a Millipore ion exchange still, and (5) the wafer surface is blown dry with dust-free nitrogen gas and the pieces are hermetically sealed until used.

Reagent grade toluene (Riedel-de Haën) was distilled over sodium metal and passed through a Millipore filter prior to use.

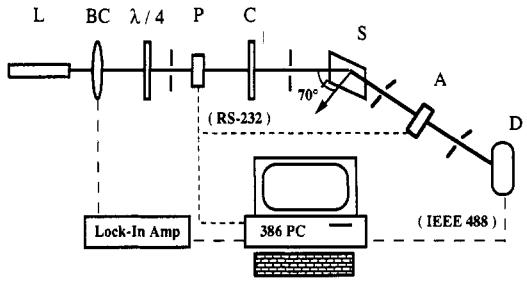

Figure 2. Schematic of the null ellipsometer employed in the adsorption studies. Stepping motors on the polarizer (P) and analyzer (A) are controlled via an RS-232 computer interface. The photodiode detector (D) is read through a lock-in-amplifier (EG&G Model 5210) coupled to a beam chopper (BC) and controlled through an IEEE-488 interface. Other components used are a helium–neon laser (L), a quarterwave plate (λ/4), compensator (C), and sample cell (S). For the results in this study, all experiments were performed at an angle of incidence of 70°.

Adsorption experiments were performed using copolymer solutions with concentrations up to and slightly exceeding 1.00 mg/mL. Control experiments with pure polystyrene at this concentration showed no evidence of adsorption under the conditions employed. Dynamic light scattering was used to check for the existence of micelles in the copolymer solutions; a description of the apparatus and procedure employed can be found in the literature.[21] No micelles were detected even at concentrations of 2.0 mg/mL, which is roughly twice the highest concentration used in our experiments.

Ellipsometry. The technique of null ellipsometry was used. This is an optical technique which relies on the fact that the state of polarization of light is altered upon reflection from a surface. On the basis of model calculations using Fresnel theory, one can obtain real time information about the optical thickness (adsorbed amount) of the adsorbing polymer film. In optimal cases it is possible to simultaneously determine the film thickness and index of refraction of the layer. However, in many cases the low contrast polymer, solvent, and substrate can be a serious problem for ellipsometry.

All measurements made were done using a homemade computer-controlled null ellipsometer is a horizontal arrangement (Figure 2). The optical train sequence consists of a polarizer, a compensator, the sample, and an analyzer (PCSA) sequence. The angle of incidence was kept fixed at a value of 70.00° within an accuracy of 0.01°. With a motorized linear polarizer (P_1) and a compensator it is possible to generate a state of elliptical polarization that when reflected becomes linearly polarized light; such light can be extinguished by the analyzer, a second motorized linear polarizer (P_2). The intensity of light passing through the second polarizer may be monitored using a photodiode while computer control of the polarizers allows an automated search for the null settings. Readings on the polarizers yield the ellipsometric angles Ψ and Δ: $\Psi = P_2$ and $\Delta = 2P_1 + 90°$. These angles contain information about the relative attenuation and phase shift of the component waves perpendicular (s-wave) and parallel (p-wave) to the plane of incidence.[22]

The trapezoidal sample cell was constructed by Hellma and has stress-free entrance and exit windows which are fixed at 70.00°. A clean silicon wafer was placed in the cell, which was then filled with 60 mL of freshly distilled and filtered toluene. A thermostat provided thermal control so that all runs were performed at 20.0 ± 0.1 °C. Upon establishment of the baseline signal, 20 mL of polymer solution (precooled to 20 °C) was injected with stirring into the glass cell, and the ellipsometric angles were monitored with time. Control experiments with toluene and pure polystyrene showed no indications of adsorption.

Surface Force Measurements. The interaction between triblock copolymer layers adsorbed onto a mica surface was studied using the surface force apparatus (SFA).[23-25] This technique uses multiple-beam interferometry to measure the distance between two back-silvered mica sheets in a crossed cylinder configuration to within ±3 Å. Freshly cleaved mica surfaces were used as substrates onto which the polymer chains were allowed to adsorb. The force between the adsorbed polymer layers at a given intersurface separation is determined directly to within ±0.1 μN by measuring the deflection of a spring bearing one of the mica sheets as the surfaces are allowed to approach one another.

Data Analysis. As mentioned above, the unknown thickness of the adsorbed layer, d_1, and its index of refraction, n_1, can be found assuming that the polymer film is a homogeneous layer. The relationship between these film parameters and the ellipsometric angles can be expressed as

$$e^{i\Delta} \tan \Psi = R_p/R_s = F(n_k, d_k) \quad (2)$$

Here, n_k and d_k refer to the indices of refraction and the thicknesses of each layer present (solution, polymer, silicon dioxide, and silicon). R_p and R_s represent the overall reflection coefficients for the basis p- and s-waves. Measurement of the two independent quantities Ψ and Δ can allow for the solution of the only two unknowns, the polymer layer thickness, d_1, and its index of refraction, n_1.

Due to the transcendental nature of eq 2, it is not possible to obtain a direct solution for n_1 and d_1. Iterative numerical schemes are needed, and we proceed as follows: knowing that the index of refraction of the adsorbed film must lie within the range of the pure solvent and the pure polymer, a reasonable starting value for n_1 may be assumed. The Fresnel reflectivity coefficient for each interface can then be determined. Based on the known value of the silicon oxide layer thickness, the complex overall reflectivity coefficient can be determined using matrix techniques.[26] Equation 2 can then be cast in terms of a quadratic equation for d_1, the unknown film thickness. Solution of this equation generally yields a complex number because the assumed index of refraction is incorrect. However, by iterating in n_1, the point at which the imaginary part of d_1 passes through zero may be found.

With a consistent set of values for n_1 and d_1, the amount of adsorbed polymer (mg/m²) can be calculated from

$$A = d_1 c_1 = d_1(n_1 - n_0)/\left(\frac{dn}{dc}\right)_0 \quad (3)$$

Here, c_1 is the mean polymer concentration within the layer, n_0 represents the index of refraction of the polymer solution, and $(dn/dc)_0$ is the change in the refractive index of the solution with polymer concentration. Weight averages of the two homopolymer values were used in determining $(dn/dc)_0$ for the copolymers.[27,28] Although a separate determination of n_1 and d_1 is difficult due to the small differences in index of refraction of the polymer and solution, the product $n_1 d_1$ is an invariant of the adopted layer model. The adsorbed amount, A, also proves insensitive toward which type of concentration profile near the wall is assumed, step, parabolic, or exponential,[20] and we therefore focus our attention on this quantity in the following discussion.

In the results which follow the grafting density has been calculated from

$$\sigma = \frac{A\ (\text{mg/m}^2)}{M_w\ (\text{mg/mol})} N_A\ (\text{chains/molecule}) \times 10^{-18}\ \ (\text{m}^2/\text{nm}^2) \quad (4)$$

which is the inverse of the area per chain. Accordingly, the interaction spacing is found from $D = (1/\sigma)^{1/2}$.

Results

Many of the salient features of the adsorption experiments are demonstrated in the graph of Figure 3, which shows the adsorption of the PEO/PS(45K)/PEO triblock material and its subsequent displacement by the PEO homopolymer. The fact that control experiments with polystyrene showed no signs of adsorption demonstrates that the copolymer is adsorbed by the PEO blocks. Consequently, the block copolymer is rapidly displaced by a layer of PEO homopolymer which adsorbs in a relatively flat conformation; this leads to the observed drastic decrease in the adsorbed amount.

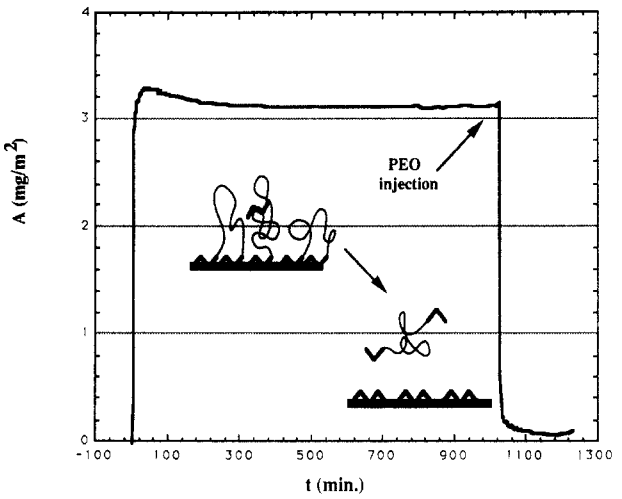

Figure 3. Triblock adsorption experiment. The end-attaching triblock copolymer rapidly adsorbs upon injection into the cell. Subsequent displacement by PEO homopolymer demonstrates the entropic penalty of stretching the chains.

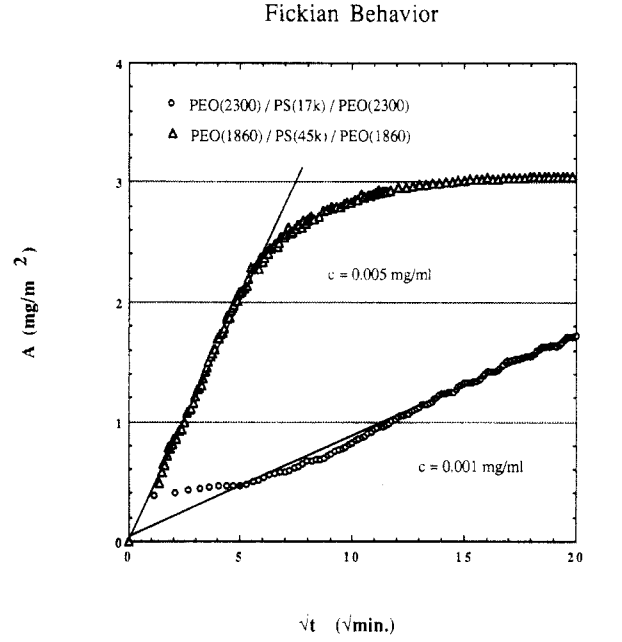

Figure 4. Short-time, low-concentration adsorption behavior. End-attaching triblock copolymers can exhibit a Fickian behavior; diffusion coefficients determined from the best line fits are in agreement with direct measurements using light scattering.

Adsorption Kinetics. The kinetic behavior of the adsorption process of end-attaching copolymers can be complicated by processes of conformational rearrangement within the adsorbed layer. For instance, Leermakers and Gast first reported the existence of an "overshoot" in the adsorbed amount for a diblock system.[29] The adsorbed layer was found to undergo relaxation over time scales lasting several days. However, for short times and low concentrations these authors found that the deposition was transport limited. This is consistent with our previous findings on diblock materials.[20]

Figure 4 demonstrates the short-time behavior for two of the end-attaching triblock copolymers. The dependence of the adsorbed amount on the square root of time is indicative of a transport-limited regime where simple Fickian diffusion to the surface is the rate-limiting step. It is reasonable for dilute concentrations to take the diffusion coefficient as constant; the diffusion equation

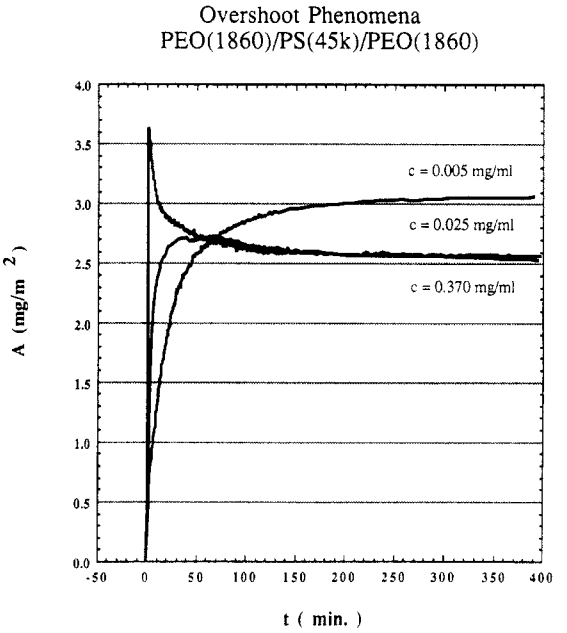

Figure 5. Kinetic overshoot effect for end-attaching triblock copolymers. On the time scale of the experiment, low solution concentrations exhibit a higher adsorbed amount than do higher solution concentrations.

may then be written as

$$\frac{\partial c(z,t)}{\partial t} = D_{AB}\frac{\partial^2 c(z,t)}{\partial z^2} \tag{5}$$

where t is time, c is concentration, and z denotes the direction normal to the surface. Assuming that the surface is initially bare and that it acts as a perfect sink (i.e., each molecule arriving at the wall is adsorbed), the boundary equations become

$$c(z=0,t) = 0 \qquad c(z,t=0) = c_0 \tag{6}$$

c_0 is the solution concentration. The solution of eq 5 subject to the boundary equations of eq 6 is given by the error function. Differentiation of this error function solution with respect to z gives an expression for the flux to the surface,

$$N_A(z=0,t) = D_{AB}\frac{\partial c(z=0,t)}{\partial z} = c_0\left(\frac{D_{AB}}{\pi t}\right)^{1/2} \tag{7}$$

which may be integrated with respect to time in order to derive an expression for the adsorbed amount on the surface as a function of time.

$$A(z=0,t) = \frac{2c_0}{\pi^{1/2}}(D_{AB}t)^{1/2} \tag{8}$$

Equation 8 demonstrates that under the stated conditions a square root of time dependence is expected.

For solutions of higher concentration, the kinetics of adsorption can be very different. We observe that both diblock and triblock materials may pass through a maximum in the adsorbed amount as the adsorption proceeds. This is demonstrated for one of the triblock materials in Figure 5 and for one of the diblock materials in Figure 6; in both cases the adsorption behavior is similar. In the lowest concentration case the adsorbed amount appears to increase monotonically and then level off at a constant value. At intermediate concentrations the adsorbed amount increases at first, reaches a maximum value, and then decreases to a constant value of the adsorbed amount which is *lower* than the value achieved for the lower concentration experiment. Finally, at high con-

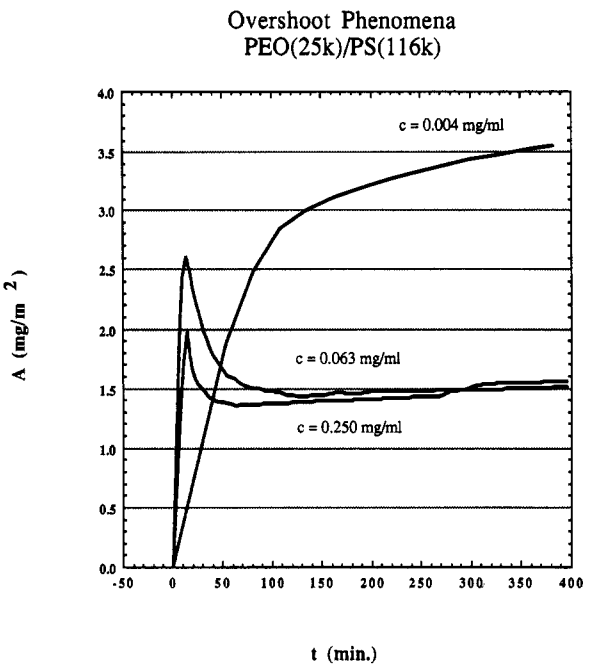

Figure 6. Overshoot effect in diblock copolymers. The adsorption behavior is very similar to that of the triblock case.

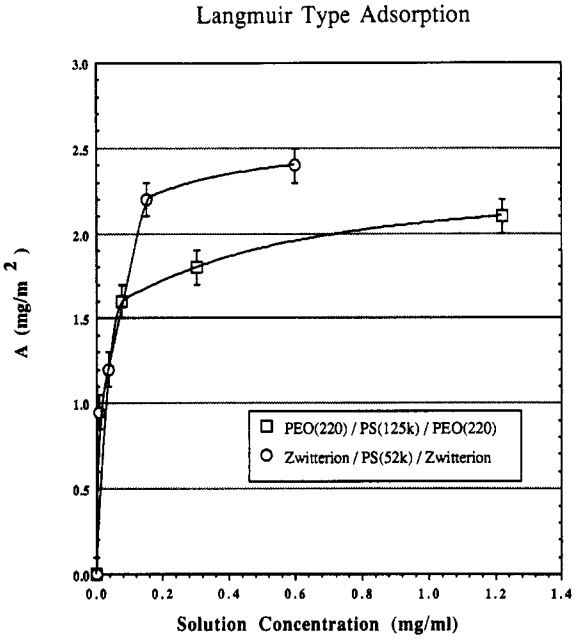

Figure 7. Adsorption isotherm for end-attaching triblock copolymers exhibiting Langmuir-like isotherms. The approach to surface saturation is clearly monotonic with increasing solution concentration.

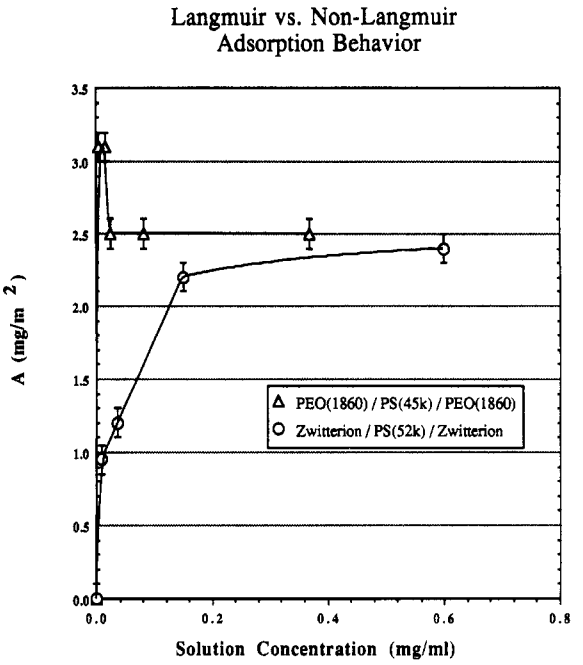

Figure 8. Comparison of Langmuir vs non-Langmuir adsorption behavior. For the PEO/PS/PEO material, a decrease in the adsorbed amount with increasing solution concentration is observed.

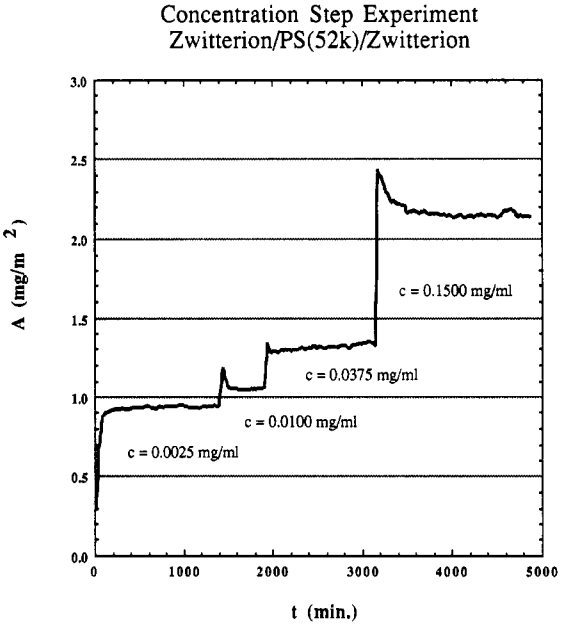

Figure 9. Multiple concentration step experiment for the zwitterionic triblock; increasing the solution concentrations within the cell leads to an increase in the adsorbed amount.

centrations, the overshoot phenomenon is rapid, and the adsorbed amount is independent of solution concentration.

Adsorption Isotherms. For two of the triblock materials studied (the zwitterion and the smallest PEO end group) the adsorbed amount was found to increase with increasing concentration. This Langmuir type adsorption is shown in Figure 7. For both materials, the approach to a plateau value where the adsorbed amount is independent of solution concentration is clearly monotonic.

The PEO/PS(45K)/PEO triblock adsorption behavior provides a stark contrast to the observed Langmuir behavior. In this case the isotherm is initially very steep; the two lowest achievable concentrations led to the same value for the adsorbed amount (3.2 mg/m^2). Solution concentrations higher than 0.015 mg/mL lead to a plateau value which is lower than the first (2.5 mg/m^2). Figure 8 shows the isotherm of this triblock copolymer along with the zwitterionic triblock isotherm for comparison. This type of adsorbed isotherm in which the adsorbed amount decreases with increasing solution concentration was first reported by Leermakers and Gast.[29] They suggested that a clustering phase transition (surface micellization) could be responsible for the observed behavior. Their conclusions were partially based on multiple concentration step experiments in which the bulk solution concentration was progressively increased.

The results for such multiple concentration step experiments for the above two triblock materials are shown in Figures 9 and 10. Figure 9 shows the results for the zwitterionic material; it is seen that as the solution concentration is increased, the adsorbed amount increases accordingly. It is also evident from this figure that the

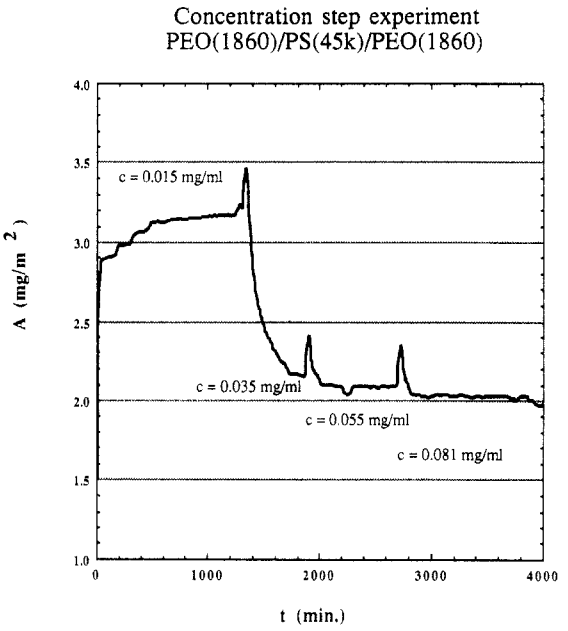

Figure 10. Multiple concentration step experiment for one of the PEO/PS/PEO triblocks; increasing the solution concentration within the cell leads to a decrease in the adsorbed amount.

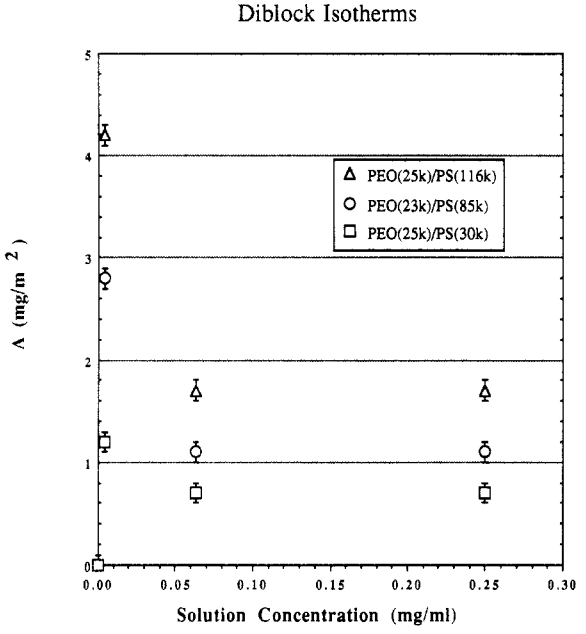

Figure 11. Diblock isotherms. Low solution concentrations lead to high adsorbed amounts; at higher solution concentrations, a lower valued plateau is found.

observable overshoot is independent of the anomalous non-Langmuir adsorption behavior. Figure 10 demonstrates that for the PEO/PS(45K)/PEO triblock, as the solution concentration is increased, the adsorbed amount falls to a lower value. It is this type of behavior which led Leermakers and Gast to conclude that the anomalous adsorption behavior represents a truly equilibrium phase transition. However, such a result in itself does not conclusively demonstrate an equilibrium effect. There exists the possibility of extremely long lived nonequilibrium states; if the relaxation rate toward equilibrium is a strong function of concentration, similar behavior would be expected.

The newly measured diblock copolymer isotherms are collected in Figure 11; again, two regimes are found. At low solution concentrations, relatively high adsorbed amounts are observed. Increasing the copolymer solution

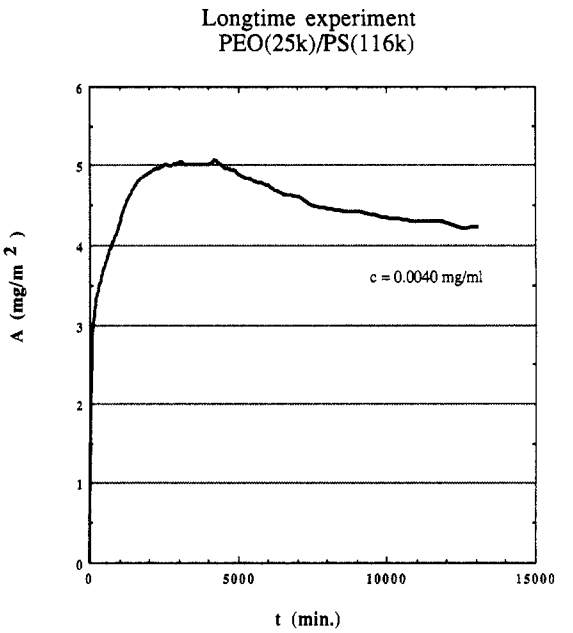

Figure 12. Long-time diblock adsorption isotherm. The adsorbed amount reaches a maximum value and remains constant for a period of 2000 min (1.4 days!); subsequently, the adsorbed amount decreases.

concentration leads to a plateau in which lower adsorbed amounts are found. However, we have performed long-time experiments which show that even at low concentrations, the surface saturation is not approached monotonically. An example of this is seen in Figure 12, which is a plot of the adsorbed amount versus time over a 9.5-day period. The existence of an overshoot on a very long time scale is clearly present! The existence of extremely long lived nonequilibrium states is consistent with previous observations on block copolymer adsorption kinetics.[29,30] Thus, at low concentrations an extremely long-time relaxation to lower adsorbed amounts cannot be excluded.

Surface Force Measurements. The interaction of end-attached layers of diblock and triblock copolymers at *saturation* surface coverage has been studied extensively using the SFA.[23-25] Here, we report data on such interactions at *partial* coverage as a function of bulk copolymer concentration. We have used the SFA to study the behavior of the PEO/PS(125K)/PEO material; this copolymer exhibits a Langmuir-like isotherm as previously noted. The results are shown in Figure 13 and reveal a strong concentration dependence of the observed forces; both the range and magnitude of the interaction increase with increasing copolymer solution concentration. This result is consistent with the observed isotherm (see Figure 7).

Discussion

The replacement experiment of Figure 3 demonstrates much of the essential physics which dictate the structure of polymer brushes. For the adsorption of the copolymer, the free energy of the system is minimized by a trade-off between the enthalpy of adsorption and the entropy of stretching the nonadsorbing block of the polymer chain. Upon injection of the PEO homopolymer, the system can realize the enthalpy of adsorption without paying an entropic penalty for stretching the nonadsorbing polystyrene blocks. The copolymer chains are thus displaced. This balance of opposing forces (enthalpy of adsorption against entropy of stretching) is what leads to the equilibrium brush structure.

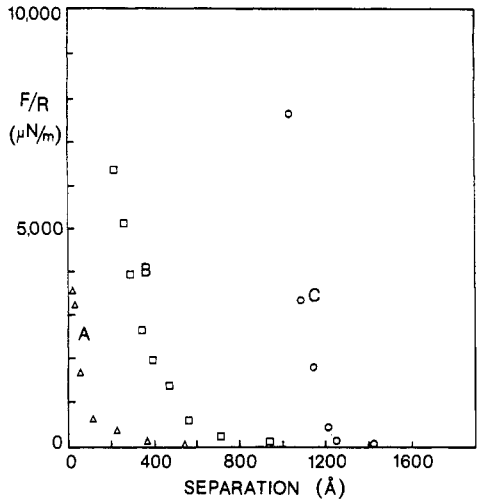

Figure 13. Force–distance profiles for the interaction of two mica surfaces bearing end-attached layers of PEO/PS(125K)/PEO in a crossed-cylinder configuration (with radius of curvature R = 10 mm). The copolymer has been adsorbed from toluene solutions of different bulk concentrations: (A) c = 0.17 mg/mL; (B) c = 0.23 mg/mL; (C) c = 1.40 mg/mL. Both the range and magnitude of the interaction increase sharply with increasing solution concentration, suggesting a significant rise in the fraction of tail conformations at the expense of loop conformations as the surface concentration increases (see also Figure 7).

Table II. Measured Interchain Spacing Compared to Overlap Spacing

material	β	D_{inter} (Å)	D_{over} (Å)	D_{inter}/D_{over}
PEO/PS(17K)/PEO	1.1	42	68	0.62
PEO/PS(45K)/PEO	2.3	57	122	0.47
PEO/PS(125K)/PEO	15.4	100	224	0.45
PEO(25K)/PS(30K)	0.6	114	96	1.19
PEO(23K)/PS(85K)	1.1	103	178	0.58
PEO(25K)/PS(116K)	1.3	114	214	0.53
PEO/PS(80K)	3.1	56	167	0.34
PEO/PS(184K)	3.5	103	276	0.37
PEO/PS(502K)	9.4	167	510	0.33

Insight into the actual structure of the adsorbed layers formed may be gained by considering the interchain spacing. As mentioned above, the interchain spacing is simply related to the grafting density through $D_{inter} = (1/\sigma)^{1/2}$ and is thus readily available from our measurements. In the cases where the adsorption isotherm had a lower plateau value at higher concentration, this lower value for the adsorbed amount is used to find σ. The Flory radius of the polystyrene block in solution may be calculated from[31]

$$R_{PS} = 1.86N_{PS}^{0.595} \quad (9)$$

and can be used to calculate the chain spacing needed for unperturbed coils on the surface to begin to touch, $D_{over} = (\pi R_{PS}^2)^{1/2}$. Table II presents a comparison of these two spacings, and it can be readily seen that, for the asymmetric diblocks and triblocks, the interchain spacing is always less than the Flory radius. Thus, in these cases a true brush structure is formed; the nonadsorbing block of the copolymer must be stretched away from the bounding surface. For the more symmetric copolymers (those with β values close to unity), the ratio to the interchain spacing to the overlap spacing decreases. Finally, for the diblock copolymer with β = 0.6, this ratio exceeds unity and it is clear that the copolymer adsorption in this case must be dictated by the size of the PEO group.

The surface force measurements also provide information as to the structure of the adsorbed layer. The differences in the onset of repulsive forces suggest significantly different structure in the adsorbed layer as a function of concentration. It is likely that at low concentration there exists a high proportion of chains adsorbed in looplike conformations, given the relatively low grafting density. For this material, as the solution concentration increases, so does the surface coverage and consequently the chains become more stretched. Thus, the population of strongly stretched tails increases and dominates the interaction onset which is seen to shift to a much longer range (see Figure 13). At a bulk concentration of 1.4 mg/mL, the onset of interaction is 1400 ± 100 Å, which can only be accounted for if stretched taillike conformations are assumed.

This marked concentration dependence of the interaction onset contrasts sharply with the behavior of diblock copolymer systems in which over a similar concentration range the observed force–distance profiles remain invariant.[8,32] However, in these highly asymmetric diblock systems the initial rise in the adsorption isotherm is very sharp so that the solution concentration range used always corresponds to the plateau of the isotherm. This is not the case with the PEO/PS(125K)PEO material; the possibility of loop or tail formation depending on surface concentration gives rise to significant changes in the range and magnitude of the observed forces.

We turn now to a discussion of the copolymer adsorption kinetics. In the diffusion-limited regime, it is possible to determine a diffusion coefficient from the slope of the adsorbed amount versus the square root of time curve. We have previously presented such results for the adsorption of diblock copolymers.[20] As indicated in Figure 4 this type of an analysis is also possible for end-attaching triblock copolymers. For the triblock containing a middle polystyrene block with a molecular weight of 17K, the diffusion coefficient obtained from the best fit line shown in Figure 4 is 9.3×10^{-7} cm^2/s; this compares well with the value 9.2×10^{-7} cm^2/s measured by dynamic light scattering. The analysis of the triblock with a 45K polystyrene middle block gives a value of 8.8×10^{-7} cm^2/s; the corresponding value measured by light scattering is 8.1×10^{-7} cm^2/s. For the third triblock copolymer, containing a middle polystyrene block with 125K molecular weight, a short-time analysis yields a value of 2.8×10^{-12} cm^2/s for the diffusion coefficient; the directly measured value is 4.1×10^{-7} cm^2/s. We interpret this large discrepancy in the latter case as meaning that the size of the PEO blocks is too small to ensure that each molecule reaching the wall is adsorbed. That is, in this case there is a certain sticking efficiency associated with the copolymer adsorption even at very low surface coverage and the substrate does not act as a perfect sink.

The overshoot phenomena found in our experiments appears to be a very general effect; it is observed for both diblocks and triblocks. Recently, a theory of adsorption kinetics capable of describing overshoot and oscillatory phenomena has appeared.[33] This model was motivated by the observation of permeation effects in biological cells. In this model, as the adsorption process begins, desorption is not allowed. That is, a time delay, τ, is invoked during which only adsorption takes place. Each adsorbed polymer is thus assumed to require the period τ to undergo conformational rearrangement to a state where desorption is possible. After this delay period both adsorption and desorption are possible. The authors develop their model explicitly for the case where the reservoir concentration is coupled to the surface concentration and present a numerical solution to the governing nonlinear equations. We present here a simplified version of this theory in which

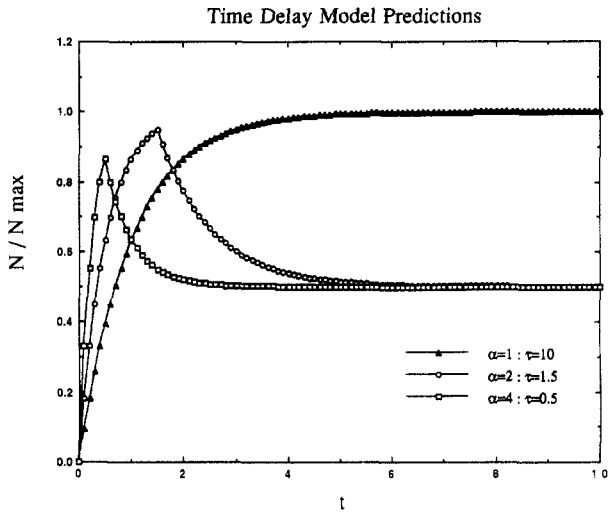

Figure 14. Predictions of the time delay adsorption model. The equilibrium adsorbed amount in all cases is $0.5N_{max}$. Long time delays lead to a saturation at N_{max} prior to the eventual decay to equilibrium.

the reservoir concentration constant (this is justified for our experimental conditions).

At high concentrations the adsorption process is no longer transport limited. Usually this type of behavior is interpreted in terms of a simple Langmuir kinetic equation. This is also the case for our time delay model where we take

$$dN/dt = k_a C_b (N_{max} - N) \quad (t < \tau) \tag{10}$$

and

$$dN/dt = k_a C_b (N_{max} - N) - k_d N \quad (t > \tau) \tag{11}$$

Here, N represents the number of occupied adsorption sites, N_{max} is the maximum number of such sites on the surface, t is time, C_b is the constant reservoir (bulk) concentration, and k_a and k_d represent adsorption and desorption rate constants. The solution to the above set of equations is

$$N/N_{max} = 1 - \exp(-\alpha t) \quad (t < \tau) \tag{12}$$

$$N/N_{max} = \frac{K}{K+1} + \left(\frac{N(\tau)}{N_{max}} - \frac{K}{K+1}\right) \exp\left\{-\alpha \frac{K}{K+1}(t-\tau)\right\} \quad (t > \tau) \tag{13}$$

In eqs 12 and 13, $\alpha = k_a C_b$ and $K = k_a C_b / k_d = \alpha / k_d$. The two time regions cross over smoothly at $t = \tau$ when $N = N(\tau)$.

At this point it is noteworthy to point out that the above model predicts a purely Langmuir isotherm. This is evident by taking the limit of eq 13 as t goes toward infinity; we are left with

$$N/N_{max} = \frac{K}{K+1} \quad (t \to \infty) \tag{14}$$

which shows that the equilibrium coverage is dictated by the parameter K. This parameter increases with increasing reservoir concentration and thus so does the equilibrium adsorbed amount. For large values of K (high concentrations), N approaches N_{max}; the surface becomes saturated.

The predictions of the time delay model outlined above are shown in Figure 14. In the calculations presented we have chosen our parameters (K, α, and τ) to mimic what we observe experimentally. It can be seen that at low concentrations (low α) and with a long time delay, the surface will saturate at N_{max}. Eventually, the coverage must decrease to the equilibrium value. At higher concentrations if the time delay decreases, then the overshoot passes quickly and the equilibrium coverage is obtained relatively rapidly. The behavior of the time delay model shown in Figure 14 can be compared with the experimental results of Figures 5 and 6; it is seen that the qualitative behavior of the adsorption kinetics is captured by this simple model.

While the above model cannot truly yield insight into the detailed mechanism of the conformational rearrangement, we present the following tentative interpretation. It is well known that one of the most salient features of polymer adsorption is that it is nearly impossible to desorb polymers by dilution but that exchange against other polymers or low molecular weight materials is possible.[34] Thus, we interpret desorption in the model as a replacement process whereby chains of unfavorable conformation become displayed by chains of lower stretching energy. At higher concentrations more chains are available in the solution which can serve to replace chains in the adsorbed layer, and the relaxation to an equilibrium structure is thus faster than in the low-concentration case.

Implicit in our physical picture of the equilibration process is the notion of *cooperativity*. It is hypothesized that the conformational relaxation process is not dictated by either free-chain penetration or single-chain desorption kinetics. No single rate-limiting step is supposed; this view is distinct from that proposed for the case of homopolymer adsorption where chain desorption is rate-limiting.[35]

The scaling behavior of the adsorbed amount lends support to the interpretation of the plateau in the observed diblock isotherm as the true equilibrium value. In Figure 14 the diblock scaling behavior of σ versus the reciprocal of the adsorbing block size is shown. The slope of this graph (approximately 2) is consistent with previously reported results for PEO/PS diblocks adsorbing onto a mica surface.[18] Additionally, the two diblocks with the same head size (i.e., PEO(25K)/PS(30K) and PEO(25K)-PS(116K)) fall precisely on top of one another. This is *not* the case when the adsorbed amounts observed at low solution concentrations are used; these values do not show the constant area/molecule which is expected for the symmetric/moderately symmetric copolymers with identical head size. This implies that the low-concentration values which are observed on the time scales of our experiments are nonequilibrium effects. The existence of extremely long lived nonequilibrium states for polymers adsorbed onto a solid surface from dilute solution has been previously observed in both experimental[36,37] and theoretical studies.[38,39]

The scaling behavior of the triblock materials is very different from the scaling behavior found for the diblocks. We find that the triblock copolymers in the moderately asymmetric range do not scale with the inverse of the adsorbing block size. In fact, for the two triblocks which fall into this category based on their β values, we find that the grafting density actually decreases with increasing $1/N_A$. This behavior prompted an attempt to scale the triblock materials according to the tail-dominated mechanism, that is, against $1/\beta^2$. The results are shown in Figure 15, where it is seen that a very strong correlation exists.

Although we have obtained only three data points for PEO–PS–PEO triblock copolymers, we point to the fact that the zwitterionic material exhibits a surface saturation which is close to but less than the value of the PEO/PS-

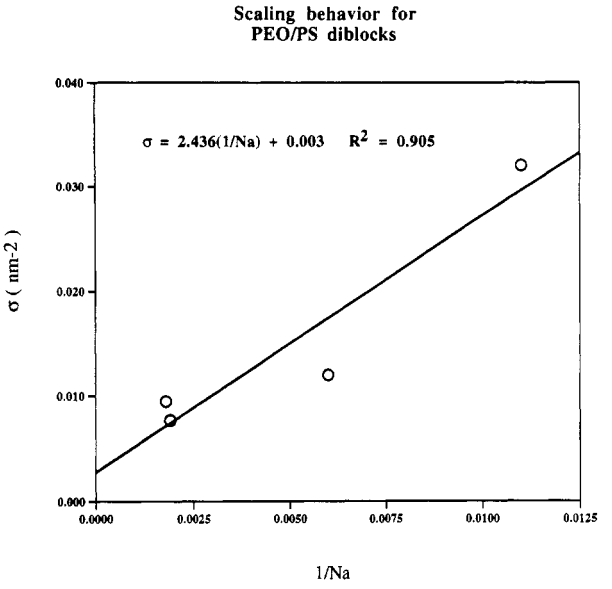

Figure 15. Scaling behavior of symmetric and moderately symmetric diblock copolymers. The grafting density is proportional to the inverse of the adsorbing block size.

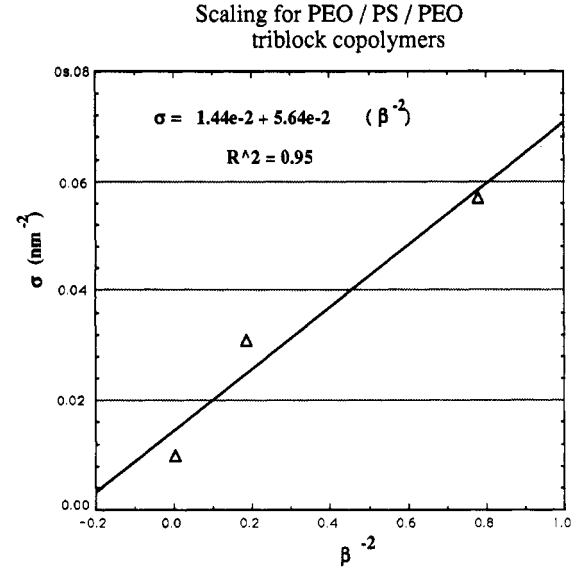

Figure 16. Scaling behavior for moderately symmetric to asymmetric triblock copolymers. Materials scale according to a dominant nonadsorbing block interaction mechanism.

(45K)/PEO. This is consistent with the tail-dominated mechanism; the zwitterionic material has a nonadsorbing middle block which is slightly larger (a molecular weight of 52K) than the PEO/PS(45K)/PEO triblock.

Conclusions

Several conclusions may be drawn from the present study but the most striking is the strong effect that the copolymer architecture plays on the equilibrium structure of the adsorbed polymer layer. We find that, as expected, diblock copolymers which are symmetric to moderately symmetric obey the scaling law for the surface coverage which was proposed in the theory of Marques and Joanny (i.e., $\sigma \propto 1/N_A$). However, we find that for triblock copolymers of comparable asymmetry the surface coverage scales according to the relationship $\sigma \propto 1/\beta^2$; this implies that moderately symmetric triblock copolymers behave like highly asymmetric diblock copolymers. In other words, nonadsorbing block interactions play an important role in determining the adsorption behavior of end-attaching triblocks over a wide range of the asymmetry variable β. This tail-dominant mechanism is further supported by a comparison between two triblocks containing nearly the same size middle block but very different end groups. For these two materials, nearly the same adsorbed amount is found; the material with the slightly larger nonadsorbing block gives a slightly smaller adsorbed amount. This difference in the adsorption behavior of the triblock and diblock materials is a striking example of how chain configuration can dictate chain conformation.

The fact that end-attaching triblock copolymers are indeed capable of forming brush structures has been clearly demonstrated. This is shown in the results of Table II, where it is seen that the adsorbed chains are confined to regions smaller than their Flory radius. The results from the surface force measurements also confirm the existence of a brush structure. Additionally, replacement experiments such as the one shown in Figure 3 demonstrate that the polymer chains are both stretched and tethered to the surface.

Another fascinating feature of our experiments is the observation of extremely long lived nonequilibrium states. We interpret the low solution concentration isotherm values as representing nonequilibrium states based on two facts. The first is that for diblocks the grafting densities obtained from these low-concentration values do not scale according to theory; however, values obtained from the plateau found at higher concentrations do scale correctly. The second fact which leads us to the above conclusion is the existence of a definite overshoot during long-time experiments at low concentrations. Our findings also indicate that the observation of these long lived nonequilibrium states and the accompanying non-Langmuir isotherm are found for block copolymers in which the adsorbing block size is relatively large; for small adsorbing block sizes, these phenomena are not present.

On the basis of these observations we propose a simplified version of a recent theory of adsorption. This model is not capable of providing a detailed molecular mechanism; however, it is capable of qualitatively describing much of the experimentally observed behavior.

References and Notes

(1) Napper, D. H. *Polymeric Stabilization of Collodial Dispersions*; Academic Press: London, 1983.
(2) Soane, D. S.; Martynenko, Z. *Polymers in Microelectronics*; Elsevier Science Publishing: New York, 1989.
(3) Reiter, G. *Phys. Rev. Lett.* **1992**, *68*, 75.
(4) Redon, C.; Brochard-Wyart, F.; Rondelez, F. *Phys. Rev. Lett.* **1991**, *66*, 715.
(5) Brochard-Wyart, F.; Daillant, J. *Can. J. Phys.* **1990**, *68*, 1084.
(6) Halperin, A.; Tirrell, M.; Lodge, T. P. *Adv. Polym. Sci.* **1992**, *100*, 31.
(7) Dorgan, J. R.; Stamm, M.; Toprakcioglu, C. *Polymer* **1993**, *34*, 1554.
(8) Dai, L.; Toprakcioglu, C. *Macromolecules* **1992**, *25*, 6000.
(9) Flory, P. J. *Principles of Polymer Chemistry*; Cornell University Press: Ithaca, NY, 1953.
(10) Alexander, S. *J. Phys. (Fr.)* **1977**, *38*, 977.
(11) Alexander, S. *J. Phys. (Fr.)* **1977**, *38*, 983.
(12) de Gennes, P.-G. *Macromolecules* **1980**, *13*, 1069.
(13) de Gennes, P.-G. *Macromolecules* **1981**, *14*, 1637.
(14) Milner, S. T. *Science* **1991**, *251*, 905.
(15) Marques, C. M.; Joanny, J. F. *Macromolecules* **1989**, *22*, 1454.
(16) Evers, O. A.; Scheutjens, J. M. H. M.; Fleer, G. J. *Macromolecules* **1990**, *23*, 5221.
(17) Evers, O. A.; Scheutjens, J. M. H. M.; Fleer, G. J. *J. Chem. Soc., Faraday Trans.* **1990**, *86*, 1333.
(18) Guzonas, D. A.; Boils, D.; Tripp, C. P.; Hair, M. L. *Macromolecules* **1992**, *25*, 2434.
(19) Munch, M. R.; Gast, A. P. *Polym. Commun.* **1989**, *30*, 324.
(20) Motschmann, H.; Stamm, M.; Toprakcioglu, C. *Macromolecules* **1991**, *24*, 3681.
(21) Förster, S.; Schmidt, M.; Antonietti, M. *Polymer* **1990**, *31*, 781.

(22) Azzam, R. M.; Bashara, N. M. *Ellipsometry and Polarized Light*; North-Holland: Amsterdam, 1979.
(23) Israelachvili, J. N.; Adams, G. E. *J. Chem. Soc., Faraday Trans. 1* **1978**, *74*, 975.
(24) Klein, J. *Nature* **1980**, *288*, 248.
(25) Patel, S.; Tirrell, M. *Annu. Rev. Phys. Chem.* **1989**, *40*, 597.
(26) Lekner, J. *Theory of Reflection*; Martinus Nijhoff Publications: Dordrecht, 1987.
(27) Brandrup, J.; Immergut, E. H. *Polymer Handbook*; John Wiley and Sons: New York, 1989.
(28) van Krevelen, D. W. *Properties of Polymers*; Elsevier Scientific Publishing: Amsterdam, 1976.
(29) Leermakers, F. A. M.; Gast, A. P. *Macromolecules* **1991**, *24*, 718.
(30) Huguenard, C.; Varoqui, R.; Pefferkorn, E. *Macromolecules* **1991**, *24*, 2226.
(31) Parsonage, E.; Tirrell, M. *Macromolecules* **1991**, *24*, 1987.
(32) Taunton, H. J.; Toprakcioglu, C.; Fetters, L. J.; Klein, J. *Macromolecules* **1991**, *24*, 3383.
(33) Ohshima, H.; Fujita, N.; Kondo, T. *Colloid Polym. Sci.* **1992**, *270*, 707.
(34) Fleer, G. J.; Lyklema, J. In *Adsorption from Solution at the Solid/Liquid Interface*; Parfitt, G. D., Rochester, C. H., Eds.; Academic Press: New York, 1983.
(35) Frantz, P.; Granick, S. *Phys. Rev. Lett.* **1991**, *66*, 899.
(36) Granick, S. In *Physics of Polymer Surfaces and Interfaces* Sanchez, I. C., Ed.; Butterworth-Heinemann: Stoneham, MA, 1992.
(37) Johnson, H. E.; Granick, S. *Science* **1992**, *255*, 966.
(38) Adriani, P. M.; Chakraborty, A. K. *J. Chem. Phys.* **1993**, *98*, 4263.
(39) Chakraborty, A. K.; Adriani, P. M. *Macromolecules* **1992**, *25*, 2470.